A concentration-dependent endocytic trap and sink mechanism converts Bmper from an activator to an inhibitor of Bmp signaling

Rusty Kelley,[1] Rongqin Ren,[1] Xinchun Pi,[1] Yaxu Wu,[1] Isabel Moreno,[1] Monte Willis,[1] Martin Moser,[1] Malcolm Ross,[1] Monika Podkowa,[2] Liliana Attisano,[2] and Cam Patterson[1]

[1]Department of Medicine, Carolina Cardiovascular Biology Center, University of North Carolina, Chapel Hill, NC 27599
[2]Department of Biochemistry, Donnelly Centre for Cellular and Biomolecular Research, University of Toronto, Toronto, Ontario M5S 3E1, Canada

Bmper, which is orthologous to *Drosophila melanogaster* crossveinless 2, is a secreted factor that regulates Bmp activity in a tissue- and stage-dependent manner. Both pro- and anti-Bmp activities have been postulated for Bmper, although the molecular mechanisms through which Bmper affects Bmp signaling are unclear. In this paper, we demonstrate that as molar concentrations of Bmper exceed Bmp4, Bmper dynamically switches from an activator to an inhibitor of Bmp4 signaling. Inhibition of Bmp4 through a novel endocytic trap-and-sink mechanism leads to the efficient degradation of Bmper and Bmp4 by the lysosome. Bmper-mediated internalization of Bmp4 reduces the duration and magnitude of Bmp4-dependent Smad signaling. We also determined that Noggin and Gremlin, but not Chordin, trigger endocytosis of Bmps. This endocytic transport pathway expands the extracellular roles of selective Bmp modulators to include intracellular regulation. This dosage-dependent molecular switch resolves discordances among studies that examine how Bmper regulates Bmp activity and has broad implications for Bmp signal regulation by secreted mediators.

Introduction

Bmp pathways are tightly regulated at multiple levels of signaling to allow for diverse biological function. The Bmp signals that initiate target cell activation are strongly influenced by extracellular Bmp modulators (for review see Balemans and Van Hul, 2002). The extracellular cues that target these downstream Bmp signaling components to distinct endocytic pathways remain unclear. Extracellular Bmp modulators, including Bmper (Bmp-binding endothelial cell precursor-derived regulator), a member of the Kielin-Chordin–related protein subfamily, are an important component of Bmp regulation as they help control the boundaries and sensitivity of Bmp signaling during many aspects of development (Michos et al., 2004; Rentzsch et al., 2006; Choi et al., 2007). Until recently, disparate reports of Bmper serving both as a pro- and anti-Bmp factor failed to support a model that explained the dual nature of Bmper activity (Conley et al., 2000; Moser et al., 2003; Binnerts et al., 2004; Coles et al., 2004; Kamimura et al., 2004; Ralston and Blair, 2005; Ikeya et al., 2006; Rentzsch et al., 2006; Serpe et al., 2008). Simple models of the biological role of Bmper do not resolve the dissonance identified in these divergent systems.

Recent data provide support for a model in which the activity of Cv-2 is biphasic with low levels of Cv-2 promoting and high levels inhibiting signaling during the formation of the crossveins in the *Drosophila melanogaster* wing. In this system, Cv-2 was found to selectively interact with Bmp ligands and receptors in a concentration-dependent manner (Serpe et al., 2008). The present study provides further evidence that Bmper behaves in a concentration-dependent manner. Bmper enhances Bmp4-mediated Smad activation at molar concentrations below that of Bmp4 in endothelial cells. Alternatively, when Bmper concentrations exceed those of Bmp4, they internalize interdependently into an endocytic shuttle to the lysosome for their dissolution. Interestingly, we found that Noggin and Gremlin, but not Chordin, can also trigger Bmp endocytosis, suggesting

Correspondence to Cam Patterson: cpatters@med.unc.edu

Abbreviations used in this paper: ES, embryonic stem; HCAEC, human coronary arterial endothelial cell; MEC, mouse endothelial cell; MEF, mouse embryonic fibroblast.

The Rockefeller University Press $30.00
J. Cell Biol. Vol. 184 No. 4 597–609
www.jcb.org/cgi/doi/10.1083/jcb.200808064

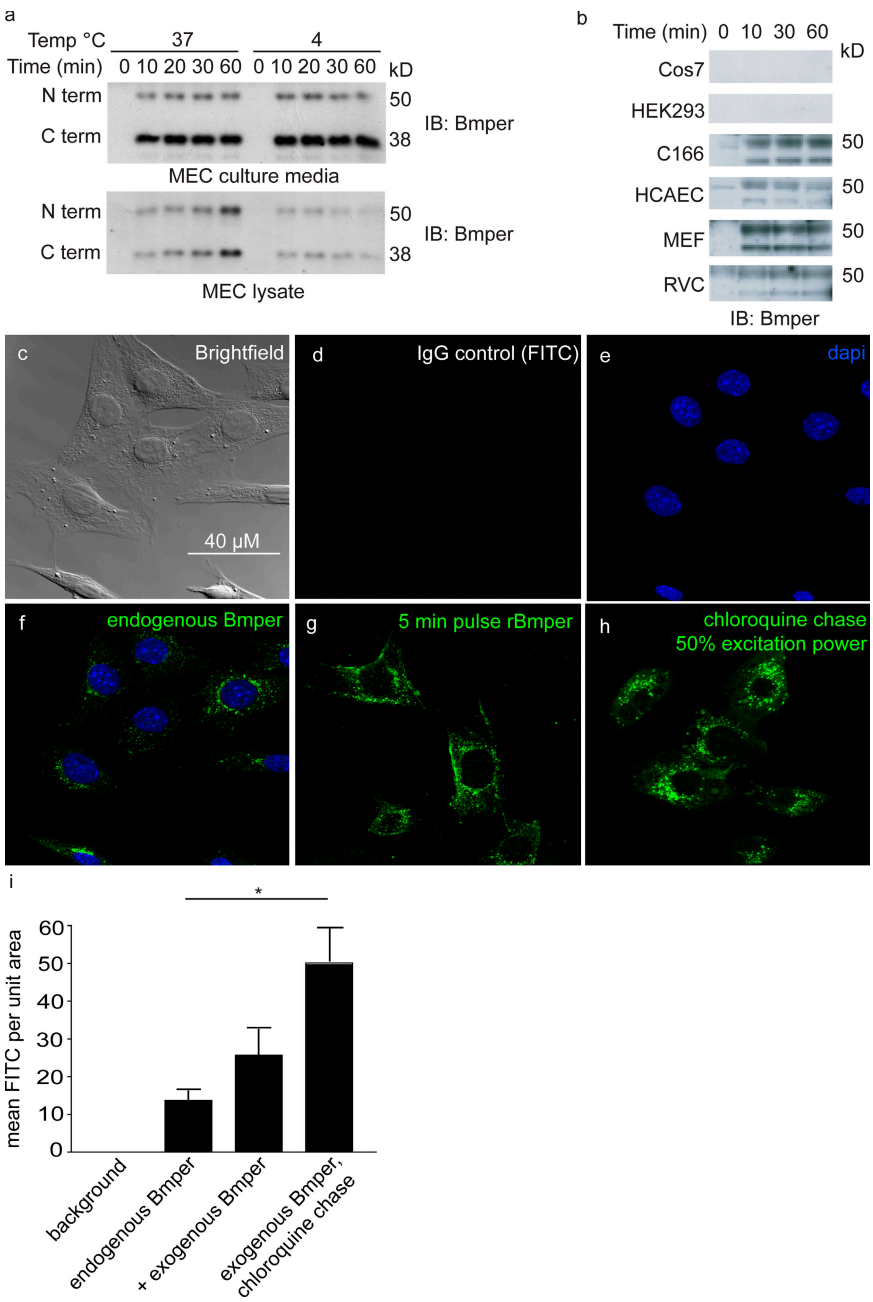

Figure 1. **Extracellular Bmper is actively internalized by selective cell types.** (a) MECs were treated with 6 nM of purified, cleaved full-length mouse recombinant Bmper at temperatures that promote (37°C) and inhibit (4°C) active transport. (b) Bmper is internalized by selective cell types, including embryonic endothelial cells (C166), HCAECs, rat neonatal ventricular cardiomyocytes (RVC), and MEFs, but not by HEK-293 or COS7 cells. Both the N- and C-terminal fragments of Bmper are presented in the Western analysis in panels a and b, whereas for clarity the N-terminal fragment only is presented in the Western analysis of all subsequent panels. (c–i) Fluorescence confocal microscopy was used to examine the intracellular localization of Bmper. MECs were treated with recombinant Bmper (6 nM). Panels c, d, and e represent images of bright field, IgG control (FITC), and nuclear staining with DAPI (blue), respectively. (f) Endogenous Bmper (DAPI overlay) was detected in MECs in a distinct punctuate perinuclear pattern that might represent the secreted form of Bmper. (g) When treated with recombinant Bmper for 5 min, a significant amount of Bmper was detected on the cell surface. (h) Bmper accumulated in large punctuate vesicles in MECs treated with Bmper and chased with media containing chloroquine. The excitation power of FITC had to be reduced by 50% to prevent the pixel saturation of fluorescent Bmper in the presence of chloroquine. (i) Graphical representation of the FITC intensity per unit area of cells treated with a pulse of exogenous Bmper and then chased with chloroquine. Fluorescent intensity is relative to cells treated with Bmper and stained with an isotype (IgG) control. The differences in the effects of endogenous Bmper, rBmper pulse, and rBmper pulse followed by chloroquine chase were statistically significant (*, $P < 0.05$) from one another and are represented by the bar in panel i. Samples were analyzed for statistics as described in Materials and methods.

that this may be a broadly applied but selective mechanism for regulating Bmp signaling.

Results

Endocytic internalization of extracellular Bmper

While probing for the effects of Bmper on Bmp6-mediated Cox2 induction (Ren et al., 2007), we discovered that recombinant Bmper (6 nM) was internalized to the cytosol when added to the culture media of endothelial cells (Fig. 1 a). As a first step to determine whether this observation represented a biologically relevant phenomenon of internalization, we answered the following questions: does Bmper cross the membrane of endothelial cells and, if so, is this through passive absorption or active transport? Is this phenomenon selective to certain cell types? Which intracellular pathway does Bmper traffic through? What are the structural requirements of Bmper protein that mediate internalization? How does Bmper internalization affect Bmp signaling?

The mouse embryo-derived endothelial cell line (mouse endothelial cell [MEC]) expresses all of the components required for appropriate Bmp signaling (Valdimarsdottir et al., 2002). To assess whether Bmper internalizes by an active process or through passive flow, we compared MECs treated with 6 nM of recombinant Bmper at temperatures that promote (37°C) and inhibit (4°C) active transport (Fig. 1 a). Bmper is processed into two fragments that remain associated by disulfide bonds (Binnerts et al., 2004; Rentzsch et al., 2006); both the N- and C-terminal fragments of Bmper were detected by Western analysis

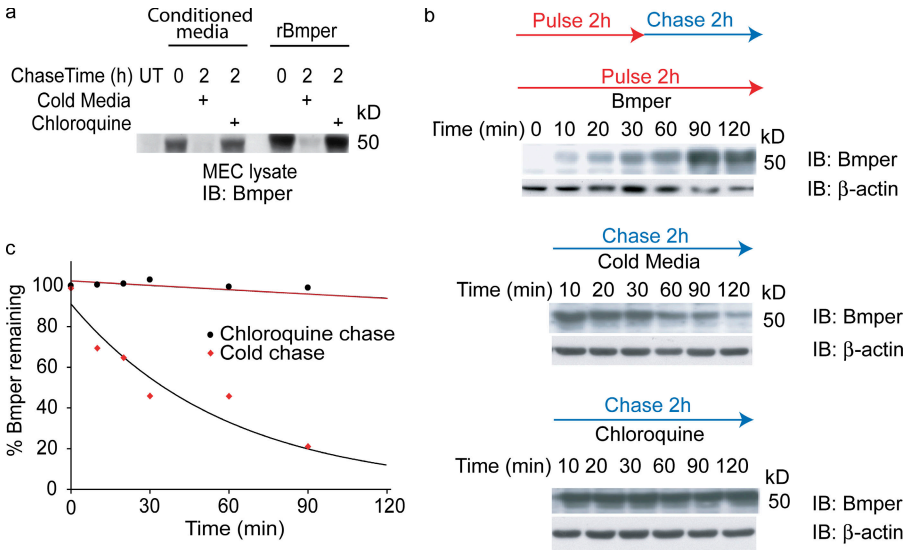

Figure 2. **Endocytic targeting of Bmper.** (a) MECs pulsed with Bmper conditioned media or purified Bmper were chased with cold media or media containing chloroquine for 2 h. (b) A Western analysis for internalized Bmper (N-terminal fragment) and activated Smad in MECs treated or pulsed with cleaved full-length rBmper (6 nM) and harvested over 2 h (top). After pulsing with Bmper, MECs were chased for 2 h with "cold" media lacking rBmper (middle) or with culture medium containing 200 µM chloroquine (bottom). (c) Graphical representation of normalized intracellular Bmper levels from the cold chase compared with the chloroquine chase from panel b.

(Fig. 1, a and b). At 37°C, Bmper internalization (as detected by its presence in cell lysates) steadily increased over time. However, Bmper internalization was barely detected at 4°C, and the small amount of Bmper detected after 20 min of treatment at 4°C was nearly eliminated by MECs after 1 h of treatment. The disappearance of both the N and C terminus of Bmper over the time course of this experiment suggest that Bmper is not only internalized but may also be further processed or degraded intracellularly. To distinguish internalized Bmper and Bmp4 from their accumulation at the cell surface, we stripped the plasma membrane with an acid wash procedure after a pulse-chase experiment (Fig. S1 a, available at http://www.jcb.org/cgi/content/full/jcb.200808064/DC1). This procedure had no effect on the detection of the internalized Bmp proteins in whole cell lysates and confirmed that the accumulation of Bmper in cell lysates is a result of endocytosis and not caused by increased cell surface affiliation. Bmper internalization was detected in endothelial cells, rat neonatal ventricular cardiomyocytes, and mouse embryonic fibroblasts (MEFs), but not by HEK-293 or COS7 cells (Fig. 1 b), indicating that the machinery required for Bmper internalization is restricted to a limited range of cell types.

We used fluorescence confocal microscopy to confirm the localization of Bmper in both untreated MECs and MECs treated with recombinant Bmper (Fig. 1, c–h). In untreated MECs, endogenous Bmper was detected at low levels with a distinct punctate perinuclear pattern. This more sensitive immunofluorescent staining likely represents accumulation of a low abundance of protein within the secretory pathway, as this form of Bmper was detectable at extremely low levels when using the same antibody for Western analysis. In contrast, a significant amount of Bmper accumulated near the plasma membrane after treating the MECs for 5 min with recombinant Bmper (Fig. 1 g). When MECs were chased with cold media (lacking recombinant protein), levels of intracellular Bmper returned to their endogenous levels (unpublished data), suggesting that internalized Bmper undergoes efficient degradation. When MECs treated with Bmper were chased with cold media containing the lysotropic agent chloroquine (Fig. 1 h), Bmper accumulated in large punctate vesicles that were clearly distinct in pattern and abundance from that seen with endogenous Bmper within the secretory pathway or after a 5-min pulse (Fig. 1 i).

To explore the possibility that internalized Bmper undergoes lysosome-dependent degradation, as suggested by the effects of chloroquine in our immunofluorescence experiments, we next compared the endocytic behavior of purified recombinant Bmper to Bmper secreted in conditioned media from HEK-293 cells transiently transfected with a plasmid encoding full-length Bmper. The HEK-293 conditioned media contained both full-length and "cleaved" Bmper, indicating that the secretory compartment of these cells is capable of cleaving the propeptide of Bmper through intracellular pH-dependent catalysis (Thuveson and Fries, 2000; Ambrosio et al., 2008; Serpe et al., 2008) or that these cells might express a yet to be identified protease capable of cleaving Bmper. The recombinant Bmper used in these studies is nearly completely cleaved. MECs were pulsed with either of the two sources of Bmper for 2 h, and then chased without recombinant Bmper but with cold media or cold media containing chloroquine for an additional 2 h (Fig. 2 a). Both recombinant Bmper (6 nM) and Bmper from HEK-293 conditioned media (6 nM) were internalized similarly by MECs during the pulse. To determine if Bmper internalizes into an endosomal transport pathway, we disrupted acidic endosomal transport during the chase phase of this experiment. Internalized Bmper was eliminated by MECs during the 2-h cold chase but, in striking contrast, Bmper levels were sustained in these cells in the presence of chloroquine. A kinetic analysis indicated that the half-life of intracellular Bmper was ~30 min and that steady-state levels were almost completely stabilized in cells treated with chloroquine (Fig. 2, b and c). These data provide further evidence of Bmper reentry from the extracellular space and indicate that Bmper is subsequently targeted for lysosomal degradation through an endocytic pathway.

Bmp4 and Bmper are reciprocally regulated through internalization

To test if other Bmp signaling components are also internalized and/or associated with Bmper-containing vesicles, we treated

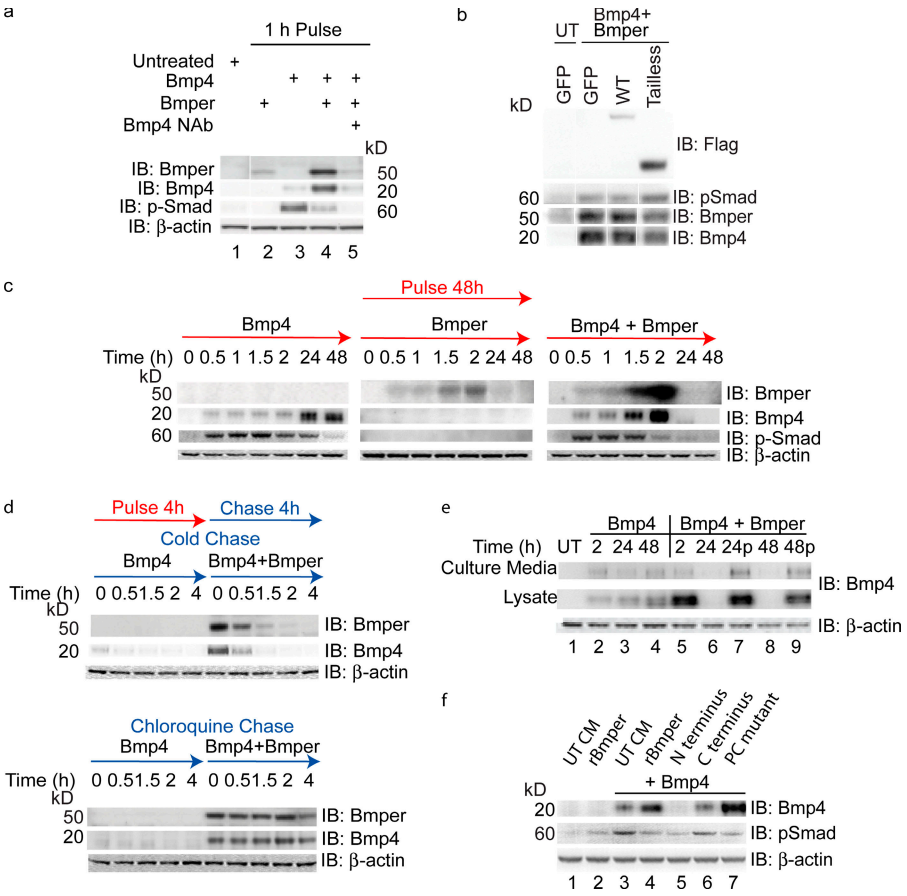

Figure 3. **Bmp4 and Bmper are reciprocally regulated by internalization.** MECs were treated with recombinant Bmper (6 nM) and/or Bmp4 (0.6 nM) and their lysates were subjected to the following analysis. (a) A Western blot showing enhanced Bmper and Bmp4 internalization in the presence of one another (lane 4). Addition of a Bmp4 neutralizing antibody prevented their internalization (lane 5). (b) MECs were infected with adenoviruses expressing GFP, wild-type Bmp receptor II (WT), or a tailless form of Bmp receptor II (Tailless) for 24 h before cotreatment with 0.6 nM Bmp4 and 6 nM Bmper for 1.5 h. (c) Kinetic analysis of the effects of Bmper (6 nM) on Bmp4 (0.6 nM) activity and Bmp4 internalization after treating MECs with Bmp4 and/or Bmper for 48 h. (d) A direct comparison of internalized Bmper and Bmp4 after a pulse with recombinant Bmp proteins and a chase with cold media or media containing chloroquine. (e) Cell lysates from MECs pulsed with Bmp4 alone (0.6 nM) and with Bmper (6 nM) for 2, 24, and 48 h were measured by Western analysis for Bmp4 in conditioned media before and after retreating the cells at 22 and 46 h (24p and 48p, respectively). (f) A Western analysis of Bmper, Bmp4, and p-Smad using lysates from MECs treated as follows: HEK-293 conditioned media from untreated cells (UT CM); untransfected HEK-293 cells spiked with 6 nM of recombinant full-length cleaved Bmper (rBmper) and/or 0.6 nM of recombinant Bmp4 (Bmp4); and conditioned media from HEK-293 cells expressing the amino fragment (N terminus), carboxy fragment (C terminus), and a proteolytic cleavage mutant of Bmper (PC mutant).

MECs with Bmper (6 nM) and Bmp4 (0.6 nM) with or without a Bmp4 monoclonal antibody that prevents Bmp4 binding to its receptor and neutralizes Bmp4-mediated Smad phosphorylation (Fig. 3 a). If Bmp ligands and Bmp receptors participate during Bmper internalization, then their respective presence or inhibition would have an effect on endocytosis. Bmp4 alone significantly activated Smad and was weakly detected in whole cell lysates. Interestingly, Bmper and Bmp4 internalization dramatically increased in the presence of one another, whereas Bmp4-mediated Smad activation was diminished in the presence of Bmper. The Bmp4 neutralizing antibody abolished Bmper-mediated Bmp4 internalization and Smad activation, suggesting that Bmper initiates Bmp4 internalization through a receptor-dependent process. To rule out the possibility that the Bmp4 neutralizing antibody disrupts the ability of Bmper to bind Bmp4, we immunoprecipitated Bmp4 in the presence of Bmper using an antibody against Myc-Bmper, both in the absence and presence of the Bmp4 neutralizing antibody (Fig. S1 b). The neutralizing antibody did not affect the ability of Bmper to bind Bmp4. These data suggest that the neutralizing antibody and Bmper bind to Bmp4 through exclusive binding sites and that the interaction of a Bmp4–Bmper complex with Bmp receptors at the cell surface is prevented by the neutralizing antibody. Accordingly, we were able to significantly reduce the amount of internalized Bmper and Bmp4 and rescue Bmp4-mediated Smad activity by ectopically expressing a tailless form of Bmp receptor II in endothelial cells (Fig. 3 b). The mutant BmprII in this construct lacks a cytoplasmic extension downstream of the kinase domain, including sequences required for endocytosis, and emulates the naturally occurring splice variant of this receptor (Lee-Hoeflich et al., 2004). It is important to note that we were able to express these proteins via adenoviral transduction with an efficiency of ~40–50% in endothelial cells, so that the effects observed by Western blotting are an underestimate of the consequences of receptor endocytosis inhibition.

To clarify the relationships of Bmp4 and Bmper on Smad phosphorylation, we evaluated the temporal effects of Bmper on Bmp4 activity using pulse and pulse-chase experiments (Fig. 3, c–e). When treated with Bmp4 (0.6 nM) alone, Smad activation was detected for at least 24 h in MECs (Fig. 3 c, left). Attenuation of Smad phosphorylation coincided with the slow accumulation of Bmp4 in cell lysates. Bmper (6 nM) alone accumulated in MEC lysates over a 2-h interval and Smad phosphorylation was not detected (Fig. 3 c, middle). When MECs were treated with both Bmp4 (0.6 nM) and Bmper (6 nM), Bmp4 internalization was markedly enhanced and accelerated with kinetics that closely paralleled those of Bmper, which in turn internalized more efficiently in the presence of Bmp4 (Fig. 3 c, right). In the presence of Bmper, Bmp4-dependent Smad phosphorylation returned to baseline much more rapidly, within 2 h (Fig. 3 c and Fig. S1, c and d). Collectively, these data indicate that Bmper regulates Bmp4 at least in part by accelerating the removal of extracellular Bmp4.

We reasoned that, similar to Bmper, internalized Bmp4 might also be sorted for lysosomal degradation as a mechanism

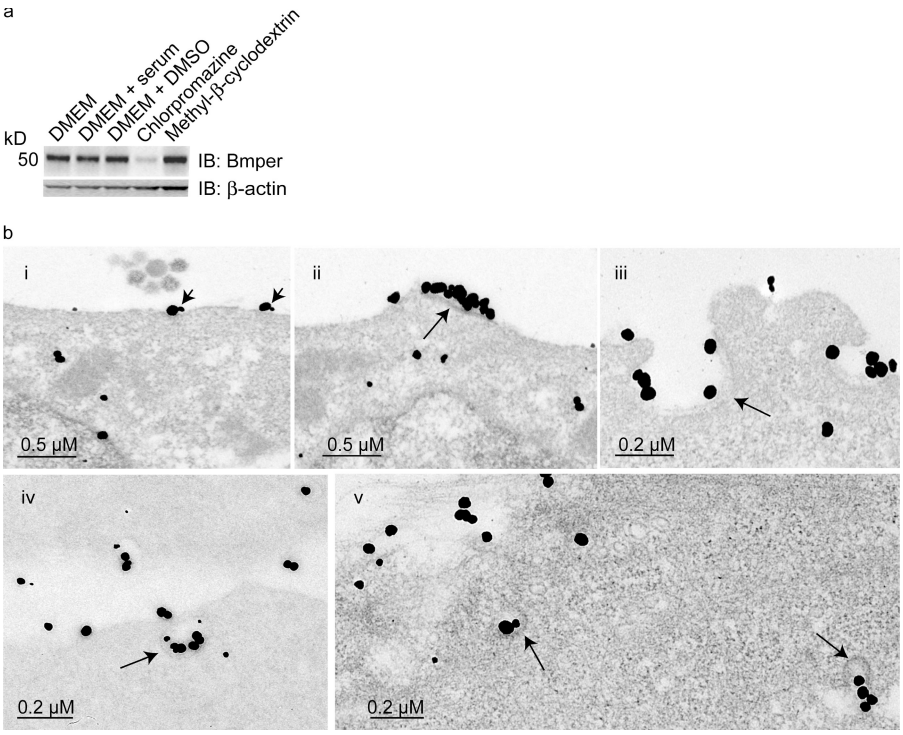

Figure 4. **Bmper and Bmp4 internalize through a clathrin-dependent mechanism.** (a) MECs were treated with 50 μM chlorpromazine to disrupt internalization into endosomes and 10 mM methyl-β-cyclodextrin to disrupt lipid raft–caveolar internalization. (b) Transmission electron microscopy sequentially captured after cotreatment of MEC with 0.6 nM Bmp4 (detected with 5-nm gold immunoparticles) and 6 nM Bmper (detected with 25-nm gold immunoparticles). Colocalization (arrows) is demonstrated at discreet locations on the cell membrane after a 5-min pulse with Bmp4 and Bmper (i and ii), coalescing along clathrin-coated invaginations (arrow) after a 30-min pulse (iii), and endocytic sorting after 1.5 h of treatment (iv and v).

to suppress its signaling. After loading exogenous proteins into cells, Bmper and Bmp4 were rapidly degraded during a chase period with cold media (Fig. 3 d, top). In contrast, chasing in the presence of chloroquine prevented lysosome-dependent degradation of both Bmp4 and Bmper with similar kinetics (Fig. 3 d, bottom), whereas the proteasome inhibitor MG-132 had no affect on Bmper or Bmp4 stability (not depicted). These data suggest that Bmper dampens the magnitude and duration of Bmp4-dependent Smad activation by restricting Bmp4 availability through endocytosis and raise the possibility (explored subsequently) that Bmper and Bmp4 colocalize during endosomal trafficking.

To determine whether the levels of extracellular Bmp are reduced by Bmper-mediated endocytosis, we measured the disappearance of Bmp4 from conditioned media and its accumulation within endothelial cells. Extracellular Bmp4 was efficiently removed from conditioned media within 24 h in the presence of Bmper (Fig. 3 e). When MECs were retreated with Bmp4 and Bmper for 2 h before 24- and 48-h harvest time points, Bmp4 internalization remained comparable to that of acute treatment. These data indicate that the extracellular pools of Bmper and Bmp4 are being depleted concomitant with endocytosis and this process does not cause loss of the cell surface machinery (that may include recycling Bmp receptors) responsible for internalizing Bmp4 and Bmper.

Both human and zebrafish Bmper are proteolytically processed into two fragments that remain associated by disulfide bonds (Binnerts et al., 2004; Rentzsch et al., 2006). To test whether proteolytic processing of Bmper affects Bmp4 internalization and signaling activity in endothelial cell culture, we compared wild-type Bmper to three mutant forms of Bmper protein: one containing only the C-terminal fragment, another containing the N-terminal fragment, and a full-length proteolytic cleavage mutant. These myc-tagged constructs were expressed in HEK-293 cells, and the conditioned media from these cells were used to treat MECs. Wild-type Bmper behaved identically to recombinant Bmper in conditioned media from untransfected HEK-293 cells (unpublished data). Likewise the C-terminal fragment had no impact on Bmp4 signaling, whereas the N-terminal fragment and the proteolytic cleavage mutant efficiently inhibited Bmp4 signaling as measured by Smad phosphorylation (Fig. 3 f). These data suggest that the N-terminal half of Bmper is required to trap Bmp4 extracellularly to prevent Smad activation through machinery that have been suggested by previous studies (Zhang et al., 2007) and that the C-terminal half of Bmper is further required to sink or internalize Bmp4 into the cell to more efficiently degrade Bmp4 and prevent signaling. Although the physiological relevance of Bmper cleavage is poorly understood, the present data suggest that Bmper proteolysis may differentially regulate Bmp activity in part by regulating its endocytosis.

Bmper and Bmp4 internalize through a clathrin-dependent mechanism

To explore the mechanism of Bmper internalization, we pretreated MECs with pharmacological agents that inhibit clathrin-dependent internalization into endosomes (chlorpromazine) or that disrupt lipid raft–caveolar internalization (methyl-β-cyclodextrin; Fig. 4 a; Di Guglielmo et al., 2003; Hartung et al., 2006). Endosomal transport was almost completely attenuated by chlorpromazine (17 μM), whereas methyl-β-cyclodextrin (10 mM; and also the caveolin-dependent inhibitors nystatin and filipin [unpublished data]) had no effect. Collectively, this study supports a clathrin-dependent, caveolin-independent mechanism for Bmper internalization. Consistent with this conclusion, there were no differences in the ability of caveolin-1 null lung endothelial cells (Lin et al., 2007) to internalize Bmp4 in the presence of Bmper compared with their wild-type

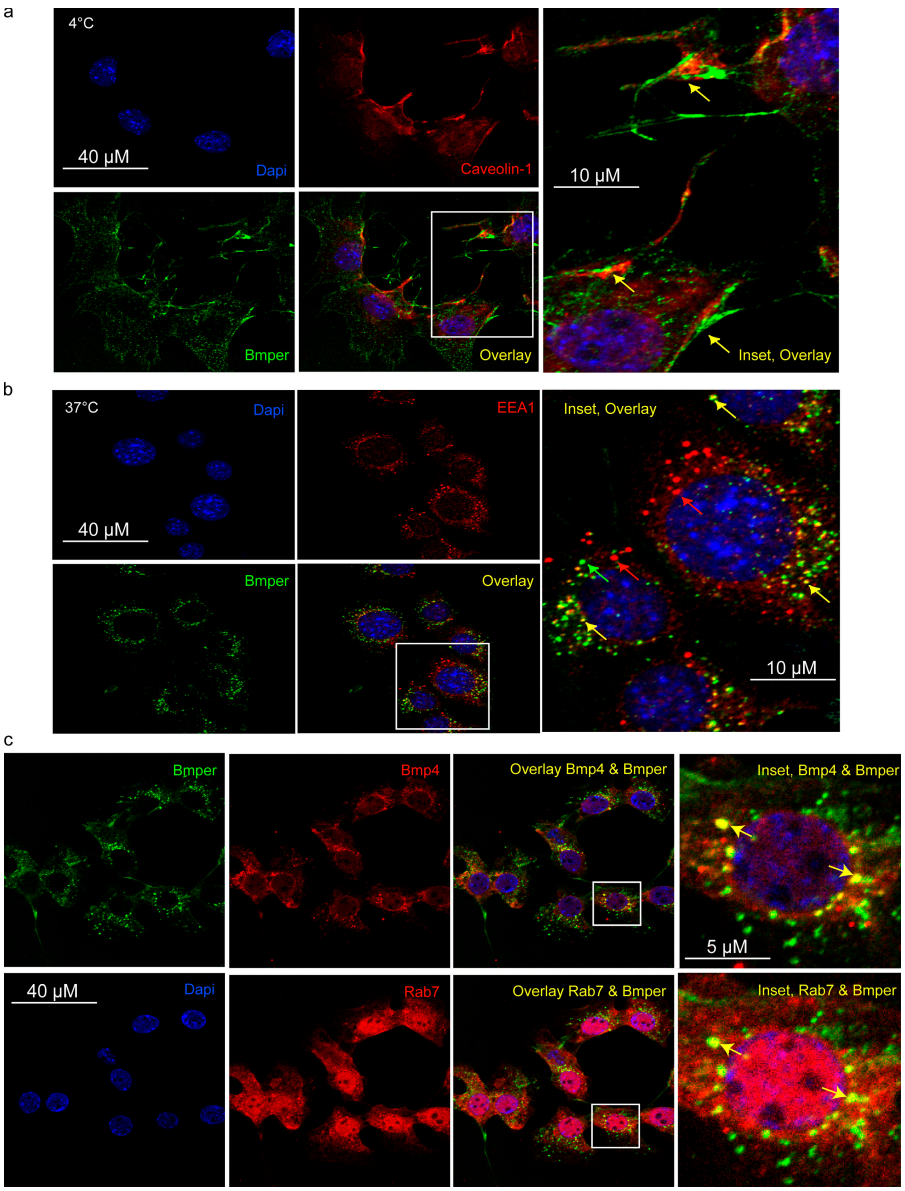

Figure 5. **Bmper and Bmp4 are shuttled to the lysosome through endocytic trafficking.** Bmper locates near a caveolin compartment at the cell surface and internalizes into early endosomes. (a) MECs cultured at 4°C and treated with Bmper (6 nM) and Bmp4 (0.6 nM) were analyzed by fluorescent immunoconfocal microscopy. A significant portion of the Bmper protein (green) appears to be localized near a membrane surface caveolin (red) compartment (arrow) and throughout filopodia. (b) After a 4°C incubation, MECs treated with Bmper (6 nM) and Bmp4 (0.6 nM) were permitted to internalize at 37°C. Bmper (green) is detected in a fraction (yellow) of the early endosomes expressing the marker EEA1 (red). (c) The same immunoconfocal analysis was used to characterize late endocytic to lysosomal translocation using the marker Rab7 (bottom, red) to colocalize with Bmper (green) and Bmp4 (red). MECs were treated with 0.6 nM Bmp4 and 6 nM Bmper for 1.5 h before fixing. Significant colocalization of Bmper and Bmp4 overlaps with Bmper and Rab7 colocalization (right panel, yellow).

counterparts (unpublished data). To explore further the pathway of Bmper and Bmp4 internalization, we performed transmission electron microscopy at selective time points (Fig. 4 b) using 25-nm immunoparticles to detect Bmper and 5-nm particles to detect Bmp4. At early time points, Bmp4 and Bmper congregated along the cell membrane (Fig. 4 b, i), presumably as they associate together with Bmp receptors. The Bmp4–Bmper heterodimers soon coalesced over a dense membrane that is characteristic of clathrin-dependent invaginations (Fig. 4 b, ii and iii). These clathrin-coated pits were subsequently visualized within the cytoplasm (Fig. 4 b, iv), and transfer of these components to mature endosomal compartments was apparent (Fig. 4 b, v, arrow). In the absence of Bmper, Bmp4 was not detected intracellularly by electron microscopy after 1.5 h of treatment. Collectively, these data are consistent with a clathrin-dependent mechanism for internalizing both Bmper and Bmp4, which is consistent with recent papers describing clathrin-dependent internalization of TGF-β and Bmp receptors (Di Guglielmo et al., 2003; Hartung et al., 2006).

Bmper and Bmp4 undergo endocytic trafficking to the lysosome

We used fluorescence confocal microscopy to further characterize the pathway by which Bmper and Bmp4 traffic (Fig. 5). MECs treated with Bmper and Bmp4 were first incubated at 4°C to capture the cell surface localization of Bmper. Bmper was located in a filamentous pattern at the cell surface, as well as in concentrated areas (possibly lipid rafts) where early endosomes begin to traffic within the cell and near filopodia (Fig. 5 a). After internalization (1-h treatment at 37°C), Bmper and Bmp4 were detected in a fraction of vesicles expressing the marker EEA1, but were not detected in caveolin-1– or phosphorylated caveolin-1–containing vesicles below the cell surface (Fig. 5 b and not depicted). This pattern is remarkably similar to reports describing cell surface localization of receptor tyrosine kinases in lipid raft compartments followed by clathrin-dependent internalization into an endocytic transport pathway (Mukherjee et al., 2006). We explored the colocalization of Bmper and Bmp4

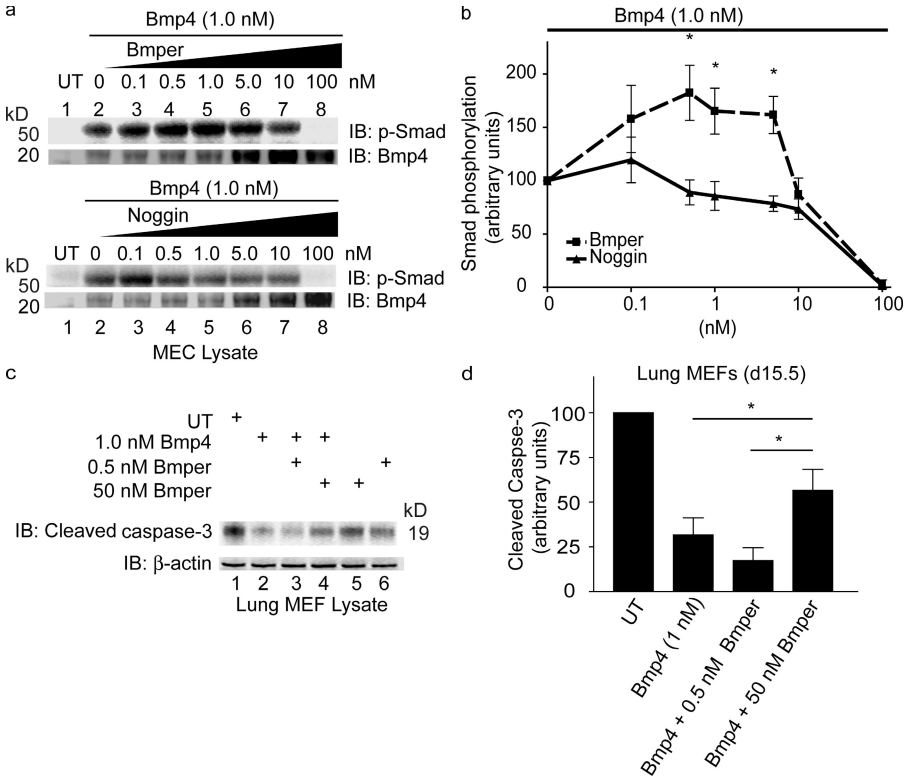

Figure 6. **Bmper regulates Bmp4 activity in a concentration-dependent manner.** (a) A representative Western blot (n = 3) of a dose–response experiment using MECs treated over a range of Bmper concentrations (0–100 nM) while holding Bmp4 constant (1 nM). Noggin was used as a positive control for inhibiting Bmp4 activity. The N-terminal fragment of Bmper is presented for the Western analysis. (b) The difference between the effects of Bmper (squares) and Noggin (triangles) on Bmp4 activity in the range of 0.1 to 5 nM was statistically significant (*, $P < 0.05$). (c) Representative Western blot showing the effects of a low (0.5 nM) and high (50 nM) molar concentration of Bmper on 1.0 nM of Bmp4-mediated cleaved Caspase-3 activity as a readout for apoptosis in primary day 15.5 lung MEFs. (d) Bar Graph showing the quantity of cleaved Caspase-3 activity from panel c. Top bar represents significant statistical difference from the untreated samples (*, $P < 0.05$). The differences in the effects of low versus high molar concentrations of Bmper on Bmp4-attenuated apoptosis were statistically significant (*, $P < 0.05$) and are represented by the bottom bar in panel d. Samples were analyzed for statistics as described in Materials and methods.

further during trafficking using Rab7, a GTPase that marks the late endosome compartment (Bucci et al., 2000; Fig. 5 c). Even at this late stage in vesicular transport, Bmper and Bmp4 remained intimately colocalized within perinuclear Rab7-expressing endosomes. The physical proximity and functional role of Rab7 in lysosomal degradation provides an additional layer of evidence that Bmper targets Bmp4 for degradation to restrict its signaling at the cellular level and is consistent with findings that a Rab7-dependent endocytic transport mechanism targets Dpp for degradation to establish a long range Dpp concentration gradient during *Drosophila* development (Entchev et al., 2000).

Bmper regulates Bmp4 activity in a concentration-dependent manner

Our discovery of a regulatory role for Bmper to regulate Bmp signaling within the endocytic pathway provides an elegant explanation for the inhibitory effects of Bmper on Bmp activity identified by multiple laboratories (Moser et al., 2003; Binnerts et al., 2004; Coles et al., 2004; Rentzsch et al., 2006; Zhang et al., 2007), but fails to reconcile other studies that indicate pro-Bmp activities of Bmper (Conley et al., 2000; Coles et al., 2004; Kamimura et al., 2004; Ikeya et al., 2006; Rentzsch et al., 2006). A recently reported concentration-dependent model helps explain both anti- and pro-Bmp activity by showing that *Drosophila* Cv-2 stimulates Bmp signaling at low concentrations and inhibits Bmp signaling at high concentrations (Serpe et al., 2008). We reasoned that a threshold effect for Bmper-dependent Bmp internalization would explain its opposing activities on canonical Bmp signaling. We tested a range of Bmper concentrations (0–100 nM) on Bmp4-dependent Smad activity and Bmp4 endocytosis, using the well characterized Bmp inhibitor Noggin as a control (Fig. 6, a and b). At molar concentrations below those of Bmp4, Bmper enhanced Smad activation, whereas at molar concentrations higher than Bmp4, Bmper attenuated Bmp4-mediated Smad activation and simultaneously triggered Bmp4 endocytosis (Fig. 6, a and b). Binding assays indicate that Bmper binds to Bmp2 with a 2:1 molar stoichiometry (Zhang et al., 2007), and remarkably it was when this molar ratio was exceeded that Bmper restricted Bmp4 signaling and triggered endocytosis of the Bmp4–Bmper complex. We also found that Noggin triggered Bmp4 endocytosis at concentrations that exceeded stoichiometric equivalence with Bmp4 (Fig. 6 a). The kinetics of Bmper- and Noggin-dependent Bmp4 internalization were similar, yet only Bmper increased Bmp4-dependent Smad signaling at below threshold concentrations. The selectivity of this endocytic mechanism for other secreted modulators of Bmp signaling is further demonstrated in the results describing Fig. 8.

We explored the concentration-dependent relationship of Bmper with Bmp4 in a biologically relevant model of Bmp signaling. At day 15.5 of embryonic lung development, the lung mesenchyme begins to regress through a Bmp4-dependent mechanism as the terminal epithelium expands into the distal airways (Bellusci et al., 1996). We found Bmper to be expressed in the supporting mesenchyme of the lung (Fig. S3, available at http://www.jcb.org/cgi/content/full/jcb.200808064/DC1), which is consistent with a previous study (Ikeya et al., 2006). Bmp4, in contrast, is expressed in the distal tips of the lung epithelium and at lower levels in the adjacent lung mesenchyme (Bellusci et al., 1996). If a concentration-dependent model for regulating Bmp signaling by Bmper is correct, then Bmper should also regulate Bmp4-mediated survival of the embryonic lung mesenchyme in a concentration-dependent manner. To test this theory, we treated

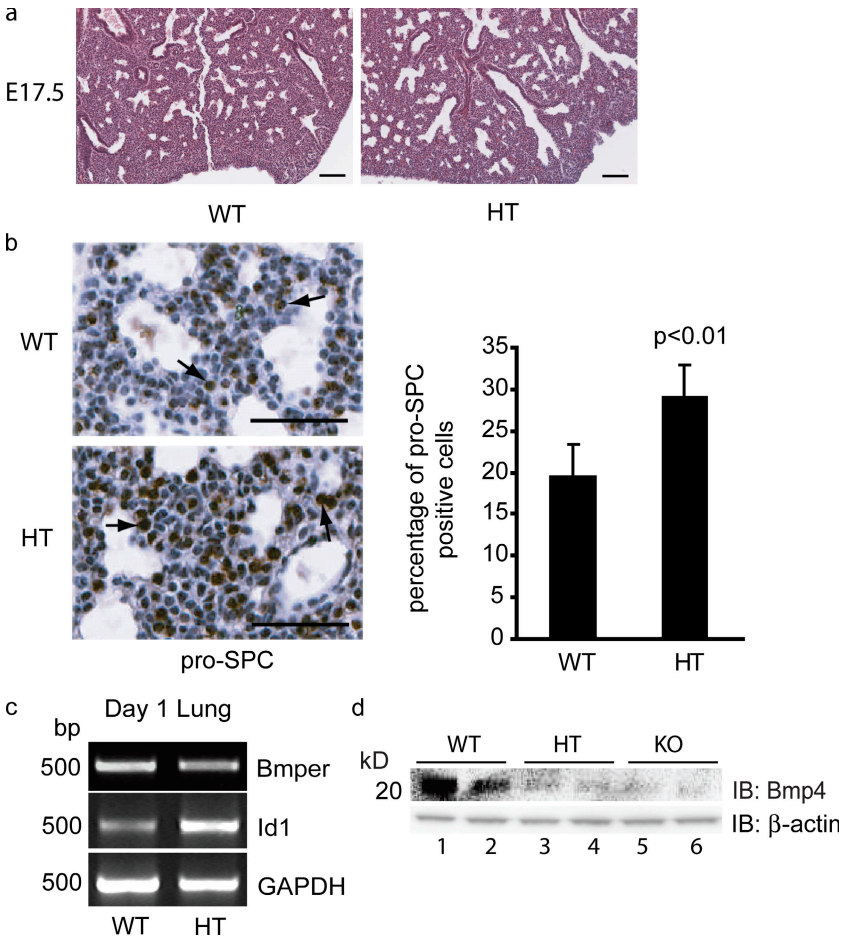

Figure 7. **Bmper inhibits Bmp signaling during lung development.** Lung development and Bmp4 activity were evaluated in wild-type (WT) mice versus mice with a heterozygous (HT) inactivation of *Bmper* at postnatal day 0. (a) Hematoxylin and eosin analysis of heterozygous lungs demonstrated delayed branching morphogenesis and inadequate expanded alveoli, which were separated by expansive interstitial mesenchyme. (b) Staining for the type II epithelial cell marker prosurfactant C (arrows). Bars, 100 µM. Positive staining is brown and counterstaining is blue. Graphical representation of the percentage of prosurfactant C–positive cells in wild-type versus Bmper het lungs. (c) Id1 mRNA expression was measured as a target of downstream Bmp activity by PCR. (d) Representative blots of endogenous Bmp4 in lysates (postnatal day 0) of lung for two individual animals each of wild-type, heterozygous, and knockout (KO) Bmper mice.

freshly isolated day 15.5 lung mesenchyme with Bmp4 (1 nM) along with molar concentrations of Bmper that enhanced (0.5 nM) or inhibited (50 nM) Bmp4-mediated Smad activation in MECs (Fig. 6 c). As anticipated, Bmp4 treatment alone protected lung MEFs from a default program of apoptosis as measured by cleaved caspase-3 (Fig. 6, c and d). At concentrations below those of Bmp4, Bmper enhanced these antiapoptotic effects of Bmp4, whereas when the molar concentration of Bmper exceeded Bmp4, Bmper attenuated Bmp4 activity, restoring apoptosis in these cells. Consistent with our concentration-dependent hypothesis, lower concentrations of Bmper alone were more protective than higher concentrations.

The fact that we were able to demonstrate a dynamic functional relationship between BMPER and Bmp4 in lung MEFS suggested the very real possibility that this novel, concentration-dependent relationship between Bmper and Bmp4 may have physiological importance, especially in the case of organ development that requires Bmp4 activity, such as the lungs (Weaver et al., 1999; Weaver et al., 2000). To test this possibility and determine the physiological importance of Bmper, we engineered Bmper-deficient mice by homologous recombination (Fig. S2, available at http://www.jcb.org/cgi/content/full/jcb.200808064/DC1).

Bmper null mice died at birth (similar to the findings of Ikeya et al., 2006), whereas heterozygotes survived. Both Bmper +/− and Bmper −/− mice exhibited widespread tissue-specific defects during embryonic development. Given the important role of Bmp4 signaling in lung development and our findings that Bmp4 and Bmper share a concentration-dependent relationship in the regulation of lung MEF survival we were particularly interested in examining the structural defects in the lungs of Bmper-deficient mice. In the perinatal lung of Bmper +/− mice, an overgrowth of mesenchymal cells (which normally express Bmper) appeared to prevent complete alveoli expansion, as indicated by smaller and fewer terminal sacs that were separated by thickened interstitial mesenchyme (Fig. 7 a). These anatomical defects are similar to lung phenotypes reported previously in Bmper-deficient mice (Ikeya et al., 2006).

Upon closer examination of the cellular and molecular features resulting from a decrease in Bmper expression, we detected several anomalies that were consistent with a "pro-Bmp" effect in the Bmper +/− lungs. At embryonic day 18.5, there was an increased ratio of type II epithelial cells to total distal cells (Fig. 7 b) as well as fewer apoptotic cells detected by TUNEL assay in *Bmper* +/− lungs compared with wild-type mice (not depicted). This abundance of interstitial mesenchymal tissue was not caused by altered differentiation or increased cell proliferation as neither of these parameters were significantly altered in Bmper +/− lungs compared with wild-type littermates. Not surprisingly, this observed phenotype was heavily localized to the distal regions of the developing lung, the region in which lung mesenchyme usually regresses if Bmp signaling

is deficient to make way for infiltrating epithelial cells that go on to form the terminal buds (Weaver et al. 1999). It is also a region where both Bmper and Bmp4 are normally expressed (Bellusci et al. 1996 and Fig. S3), suggesting that without Bmper, Bmp4 activity is allowed to signal unabated, thereby reducing the amount of mesenchymal apoptosis, a theory that is supported by our in vitro measurements of proapoptotic activity of Bmper in explanted embryonic lung mesenchymal cells (Fig. 6, c and d).

To confirm at the molecular level that the observed changes in Bmper +/− lung tissue were a result of increased Bmp signaling, we measured the amount of Id1, a downstream Bmp target (Hollnagel et al., 1999), in lung tissue of both Bmper +/− and wild-type mice by PCR (Fig. 7 c). As expected, there was an appreciable increase in Id1 expression in Bmper +/− lungs, further indicating that the reduction in Bmper expression leads to a pro-Bmp effect in this tissue. These data suggest that the failure of the lungs to mature in Bmper +/− mice is caused by sustained Bmp4 signaling in the distal region of the lung (resulting in a failure of the mesenchyme to recede) and not by a nonspecific secondary effect of delayed lung development. Collectively, these data support a tissue-specific and physiologically relevant anti-Bmp role for Bmper and are also consistent with the anti-Bmp effects of Bmper in the developing pupil wing of *Drosophila* (Serpe et al., 2008).

If increased Bmp activity in Bmper +/− mice is at least partially caused by impairment of Bmper-mediated Bmp4 endocytosis, then one would anticipate decreased cytoplasmic accumulation of Bmp4 in the cytosol of lung cells. In isolated cell preparations from mouse lung stripped of membrane, Bmp4 was found to accumulate in the cytosol of wild-type lung cells in substantial levels, but was present in markedly reduced levels in both *Bmper* +/− and −/− lungs (Fig. 7 d), indicating that Bmper is necessary for optimal internalization of Bmp in vivo, as it is in vitro. These observations, combined with the aforementioned finding of increased Bmp signaling in Bmper +/− lung tissue and our in vitro studies, indicate strongly that Bmper exerts a physiologically relevant anti-Bmp effect and supports a mechanistic model whereby BMPER regulates Bmp signaling in part by promoting Bmp endocytosis and subsequent lysosomal degradation.

Endocytosis mediated by Gremlin and Noggin but not Chordin

Discrete but overlapping developmental expression patterns of multiple Bmp regulators during patterning (Srinivasan et al., 2002; Ralston and Blair, 2005; Rentzsch et al., 2006) suggest mutually dependent interactions among these factors. The specificity of Bmper-mediated endocytosis of Bmp4 prompted us to test the effects of recombinant Chordin, Noggin, and Gremlin on Bmp4-mediated Smad activation and endocytosis to determine the extent to which this novel endocytic mechanism extends to other classical extracellular regulators of Bmp signaling. Under all conditions tested, Bmper induced Bmp4 internalization while reducing Bmp4-mediated Smad activity to a level intermediate to that of Bmp4-treated and untreated cells (Fig. 8, a and b). Consistent with previous reports of their potent Bmp inhibitory activity, Noggin and Gremlin eliminated Bmp4-mediated Smad activation, irrespective of Bmper treatment, and led to Bmp4 endocytosis (Fig. 8 b, middle and bottom). The apparent affinities of Noggin and Gremlin for Bmp4 are higher than Bmper, as they abolished Bmper internalization and more potently reduced Bmp4-mediated Smad phosphorylation. The ability of Noggin and Gremlin to induce Bmp4 internalization suggests that endocytic internalization of Bmps also accounts, at least in part, for their ability to inhibit Bmp activity. In contrast, Chordin had no effect on Bmp4-induced Smad activation or endocytosis. Although Chordin was inactive in the presence of Bmp4 alone, Bmper induced Chordin internalization. Interestingly, internalization of Bmp4, Bmper, and Chordin were attenuated when all of these factors were present simultaneously (Fig. 8 c), suggesting that higher order protein complexes may actually suppress the endocytic mechanism.

We conducted further studies to determine whether Noggin also targets Bmp4 for the lysosome and whether Bmper has this effect on Chordin (Fig. 8 c). The effects of Noggin on Bmp4 were similar to the effects of Bmper on Bmp4 (Fig. 8 c, middle), as Bmp4 was degraded during the cold chase, but not in the presence of chloroquine. The proteolytic processing of Bmp4 in the presence of Noggin was not as thorough as when Bmp4 was in the presence of Bmper, suggesting there may be subtle differences in Bmp proteolysis and possibly the kinetics of elimination elicited by different Bmp modulators. Interestingly, Noggin was constitutively internalized by the endothelial cells. This is in contrast to Chordin, which was not internalized in the presence of Bmp4, whether or not Bmper was present. However, in the presence of Bmper alone under these culture conditions (Fig. 8, b and c), Chordin was internalized and eliminated after a cold chase. Interestingly, intracellular Chordin did not accumulate after chloroquine chase. It is possible that internalized Chordin is eliminated by the cell independent of the lysosome (i.e., via proteasomal degradation) or that the kinetics of its turnover differs from Noggin and Bmper. That the intracellular trafficking of Chordin is distinct from Bmper and Bmp modulators such as Noggin and Gremlin may reflect the higher affinity of Bmper for a Bmp4–Chordin complex than it does for Chordin alone. Collectively, these data suggest a complex and competitive interplay among Bmp modulators for Bmps and underscore a generalized role for activities within the endocytic compartments among selective Bmp modulators.

Discussion

Several models have been proposed to explain the anti- and pro-Bmp mechanisms of Bmper (Coles et al., 2004). Recently, a paper using biochemical and genetic studies in *Drosophila* proposes a model where Cv-2 can enhance and inhibit Bmp signaling at low and high concentrations, respectively (Serpe et al., 2008). Dependency on concentration and proteolytic cleavage have also been reported for other extracellular modulators of Bmp activity (Larrain et al., 2001). Our data provide an additional mechanism whereby proteolysis and concentration dependency fine-tune Bmp signaling through interactions with secreted proteins.

Although both proteolytic activation and inactivation have been described for several Bmp factors, the degradation of secreted Bmps are incompletely understood. To date, limited data

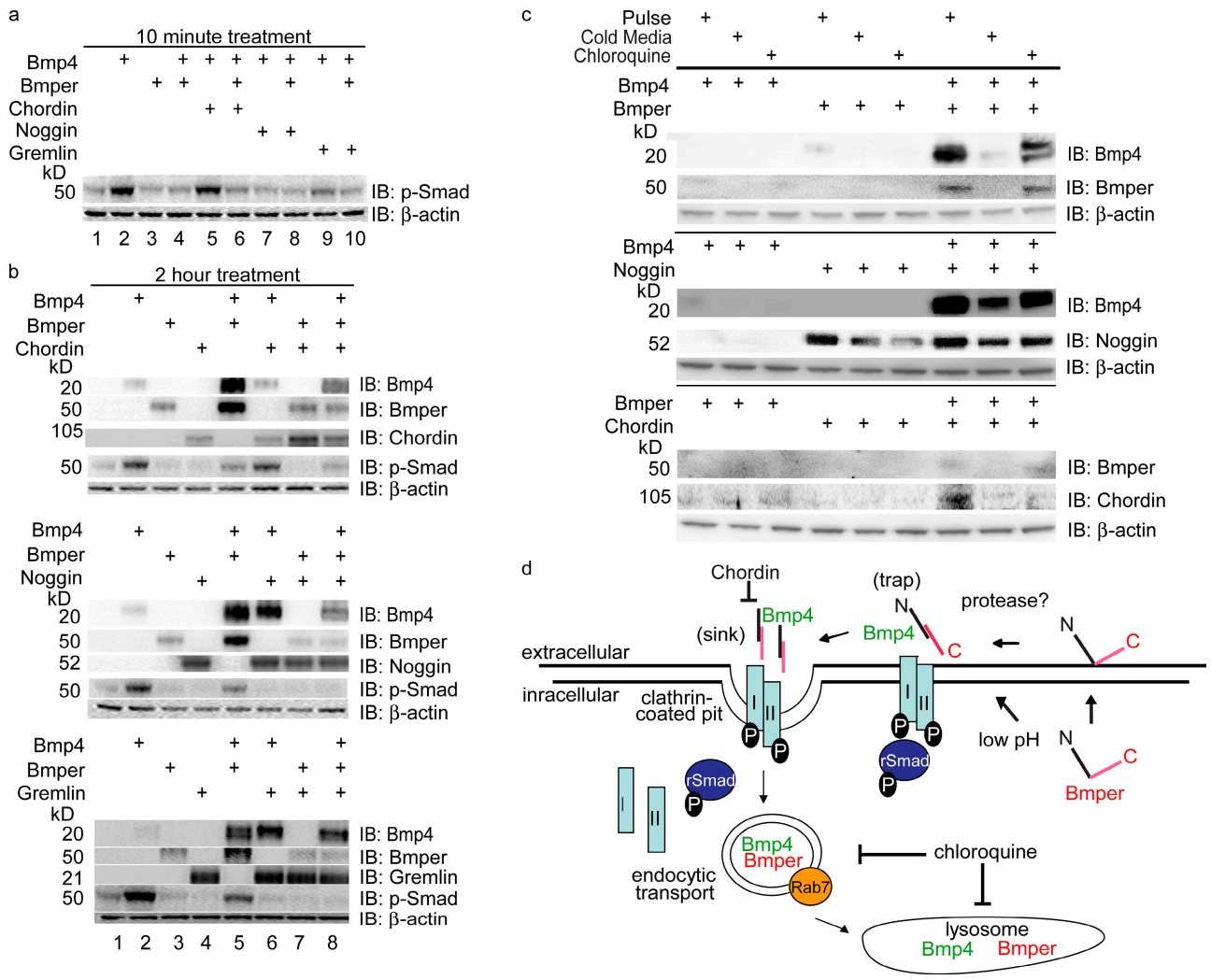

Figure 8. **Bmp4 endocytosis is mediated by Bmper, Gremlin, and Noggin, but not Chordin.** A panel of secreted Bmp factors (6.0 nM) were evaluated for their effects on Bmp4 (0.6 nM) and on Bmper-mediated Bmp4 internalization and signaling at several time points. A Western analysis showing the effects of active recombinant Chordin, Noggin, and Gremlin on the activity of Bmp4 alone or with cleaved full-length Bmper was measured 10 min (a) and 1.5 h (b) after treatment. Protein internalization and Smad activation were measured for each of these Bmp factors: Chordin (top), Noggin (middle), and Gremlin (bottom). (c) Pulse-chase experiment in MECs treated with Bmp4, Bmper, Noggin, and combinations of Bmp4 and Bmper (top), Bmp4 and Noggin (middle), and Bmper and Chordin (bottom). After treating MECs with recombinant protein(s) using the same experimental conditions and protein concentrations used in panel a, MECs were either chased with cold media or cold media containing chloroquine that lack recombinant protein(s). (d) A model of Bmper-mediated Bmp4 internalization.

are available describing Bmp degradation (Entchev et al., 2000; Degnin et al., 2004). Lysosomal- and proteasomal-dependent degradation of Bmp4 within the presecretory pathway was shown to occur after the initial cleavage step of the inactive Bmp4 precursor and before the final cleavage step that stabilizes the mature secreted form (Degnin et al., 2004). Postsecretory regulation of Dpp through an endocytic mechanism that traffics DPP to the lysosome for degradation during *Drosophila* development has also been described. The present study provides the first example of targeted intracellular Bmp degradation by a secreted regulator of Bmp signaling and indicates that this endocytic mechanism is broadly used by Bmp regulators such as Bmper, Noggin, and Gremlin to fine-tune Bmp regulation.

Indications that endocytic internalization mechanisms modulate Bmp signaling were first suggested by studies in *Drosophila* showing that a Dynamin-dependent retrieval process participates in creating an inverse gradient of the Bmp modulator Sog (a Chordin homologue), which fine-tunes concentration gradients for Dpp in the extracellular space (Srinivasan et al., 2002). Receptors for Bmp family members have also been shown to internalize through distinct endocytic pathways. In the case of TGF-β receptors, caveolin-dependent internalization mechanisms target the receptors for proteasomal degradation, whereas clathrin-dependent internalization alternatively is required for appropriate Smad activation (Di Guglielmo et al., 2003). Constitutive internalization and degradation of type I and II Bmp receptors via clathrin-mediated endocytosis, and to a lesser extent internalization of BmprII by a caveolae-dependent route, have also been established (Hartung et al., 2006). Our experimental observations extend the role of endocytic mechanisms within the Bmp signaling pathway by demonstrating mutually triggered clathrin-dependent endocytosis

of Bmper and Bmp4 and significant involvement of surface Bmp receptors in mediating endocytic sorting of Bmper and Bmp4 to the lysosome to limit the temporal boundaries of Smad activation.

The inhibitory activity of Bmper is supported by our in vivo evidence that Bmper behaves as a tissue-specific Bmp inhibitor in the developing lung of Bmper-deficient mice. The deletion of Bmper affects the distal area of the lung where Bmper is expressed in the mesenchyme, but not the proximal area where both Calcitonin gene-related peptide and Clara cells are located. These results strongly support the interpretation that the phenotype in Bmper +/− lungs is caused by local deficiency of Bmper and not by a nonspecific secondary effect of delayed lung development. The physiological anti-Bmp activity of Bmper during lung development is completely consistent with our in vitro evidence that Bmper leads to apoptosis of embryonic interstitial lung MEFs, which is normally inhibited by Bmp signaling. Whether Bmper exerts pro- or anti-Bmp activities in vivo in different models may be tissue and possibly species specific and tissue differences in the ratios of Bmper to Bmp family members likely determine whether Bmper is augmenting or suppressing Bmp signaling.

Collectively with previous biochemical and genetic studies (Coles et al., 2004; Rentzsch et al., 2006; Zhang et al., 2007; Serpe et al., 2008), a model can be developed that parsimoniously accounts for seemingly disparate observations (Fig. 8 d). At low molar concentrations, Bmper may bind Bmp4 in a manner that increases the affinity of Bmp4 for its receptors (Zhang et al., 2007), accounting for the activation of Bmp signaling that we observe under these conditions (Fig. 6 a). A recent study suggests that this occurs through a Bmp, Bmper, and Bmp receptor tripartite complex that facilitates transfer of Bmp to the Bmp receptor to account for this activity (Serpe et al., 2008). As Bmper exceeds the molar concentration of Bmp4, high affinity Bmp4 receptor binding determinants may be masked, resulting in a low affinity receptor interaction, but in any event endocytosis of both Bmp4 and Bmper is clearly triggered under these circumstances in a receptor-dependent fashion. The uncleaved form of Bmper was previously suggested to exert its anti-Bmp activity through association with components of the extracellular matrix and cell membrane (Rentzsch et al., 2006), but the present studies make clear that the uncleaved form of Bmper also enhances Bmp4 endocytosis, facilitating a Bmp4 sink through recruitment of Bmps to the cell surface. Furthermore, although the N terminus of Bmper binds Bmp4, the C terminus of Bmper is required for this endocytic mechanism; our results and those of other groups lead us to speculate that the C terminus of Bmper may facilitate endocytosis through interactions with the extracellular matrix and/or Bmp receptors. Under certain conditions, the function of trapping Bmps by Bmper can be uncoupled from an intracellular Bmp sink, and therefore endocytosis is not essential to the inhibitory activity of Bmper. The ability of not only Bmper but also Gremlin and Noggin to trigger the endocytosis of Bmp4 suggests that this is a broadly applied mechanism by inhibitors of Bmp signaling to regulate the concentration and temporal availability of Bmps as a signal regulation strategy.

Materials and methods

Antibodies and reagents

The antibodies and recombinant proteins for Bmper, Bmp4, Noggin, Chordin, and Gremlin and monoclonal anti-human Bmp4 neutralizing antibody were purchased from R&D Systems. Phosphorylated Smad and cleaved Caspase 3 antibodies were purchased from Cell Signaling Technology. QuikChange site-directed mutagenesis (Agilent Technologies) was used to modify a previously described pSecTag2 vector containing wild-type Bmper (Moser et al., 2003). W.C. Sessa (Yale University School of Medicine, New Haven, CT) provided the lung endothelial cells null for caveolin-1.

Preembedding immunoelectron microscopy

MECs were fixed with 4% paraformaldehyde/0.5% glutaraldehyde. After three washes in 0.15 M sodium phosphate buffer the cells were immunostained using a preembedding immunogold-silver procedure developed by Yi et al. (2001). 70-nm ultrathin sections were cut using a diamond knife and an Ultracut UCT microtome (Leica), mounted on 200 mesh copper grids and post-stained with Reynolds' lead citrate for 8 min. Sections were examined on a transmission electron microscope (EM-910; Carl Zeiss, Inc.) using an acceleration voltage of 80 kV and a 75-µm objective aperture. Digital micrographs were taken using an Orius digital camera (Gatan, Inc.).

Cell culture

MEFs were isolated from mouse lung at embryonic day 15.5 from wild-type mice of a mixed background (C57BL/6 and Ola 129). In brief, embryos were dissected from the mother's uterus and placed in sterile PBS in a 10-cm dish. The embryos were separated from fetal membranes (in the case of lung MEFs, lung lobes were separated from the heart and neighboring connective tissue) and placed in 1 ml of 0.25% trypsin-EDTA and a sterile razor blade was used to mince the embryos. The minced embryos were allowed to sit in the trypsin-EDTA for 10 min at 37°C and 5% CO_2 followed by neutralization in 2 ml of growth media (DME, 10% FCS, and penicillin and streptomycin with 50 µM β-mercaptoethanol). After repeatedly pipetting and disaggregating the tissue, 8 ml of growth media was added to the plates to seed the fibroblasts. On day 2, the 10-cm plates were confluent and cells in suspension were removed. The cells were passed once and then used for experimentation. MECs were cultured as previously described (Moser et al., 2003; Ren et al., 2007) and human coronary arterial endothelial cells (HCAECs; Lonza) were cultured according to the manufacturer's recommendation using EGM-2 media (Lonza).

Unless otherwise indicated, cultured cells were treated with recombinant Bmp4 (0.6 nM) and/or recombinant Bmper, Chordin, Noggin, and/or Gremlin (6.0 nM) in high glucose DME for various times to analyze the temporal effects of Bmper toward Bmp4 activity and internalization. For chase experiments, cells were pulsed with recombinant proteins and then chased with "cold" or normal DME media or media containing chloroquine for the indicated times. Active internalization was determined in cells cultured normally at 37°C versus pretreating the cells at 4°C for 45 min before treating them with recombinant proteins for up to 60 min at 4°C. Conditioned media were harvested after 48 h of transfecting HEK-293 cells using FuGENE and cDNA from wild-type Bmper or Bmper mutants. Undiluted condition media were applied to MECs, and recombinant proteins used in the mutant studies were diluted in control (untransfected) HEK-293 condition media as positive controls for internalization and Bmp signaling.

Subcellular localization

Immunolocalization was performed on untreated and treated MECs and HCAECs, fixed with 4% paraformaldehyde, permeabilized with 0.1% Triton X-100, blocked with 1% BSA in PBS, and incubated with primary antibodies, followed by incubation with Alexa Fluor secondary antibodies. Digital pictures were taken using an upright laser scanning confocal microscope (SP2 AOBS; Leica) at room temperature (at the University of North Carolina's Michael Hooker Microscopy Facility). Images were processed using LCS Lite imaging software (Leica) and Photoshop (Adobe).

Western blotting analysis

Western analysis was performed on MECs treated with recombinant proteins (all purchased from R&D Systems). In brief, blotting was performed by incubating primary antibodies (anti-Bmper [R&D Systems], anti-Bmp4 [Millipore], anti-Chordin, anti-Gremlin, and anti-Noggin [R&D Systems]). Blots were developed with an Advanced ECL kit (Thermo Fisher Scientific). Immunoprecipitation was performed using an anti-Myc antibody (Santa Cruz Biotechnology, Inc.).

RNA isolation and real-time PCR

Total RNA was extracted from cells and tissues using RNeasy kits according to the manufacturer's instructions (QIAGEN). First-stand cDNA was synthesized using 500 ng of total RNA with 200 U of Superscript II RNase H-RT (Invitrogen) in a final volume of 20 µl. The resulting products were then treated with RNase A for 30 min at 37°C and purified thereafter with Qiaquick PCR purification kit (QIAGEN). Real-time PCR was performed using the 7500 Real-time PCR system (Applied Biosystems).

Lung histology

Mouse tissues were fixed overnight in 4% paraformaldehyde/PBS and processed for paraffin embedding. Deparaffinized sections (5 µm) were treated with Antigen unmasking reagent (Vector Laboratories) for 15 min for antigen retrieval. Blocking was achieved with 2.5% horse serum in PBS for 10 min. Primary antibody (anti-GFP and anti–prosurfactant C) incubations were performed for 30 min at room temperature. Biotinylated secondary antibodies (Vector Laboratories) were added to sections for 10 min, followed by signal detection using NovaRED reagent (Vector Laboratories). Anti–prosurfactant C antibody was a gift from J. Whitsett (Cincinnati Children's Hospital Medical Center, Cincinnati, OH).

TUNEL assay

TUNEL assay was performed according to the manufacturer's instructions (Promega). In brief, paraformaldehyde-fixed and paraffin-embedding lung tissue sections were stained with fluorescein-12-dUTP (Promega). Images were acquired using a confocal microscope (Carl Zeiss, Inc.).

Target deletion of mouse *BMPER* gene

Mice deficient for Bmper were generated with standard gene targeting methods (Dai et al., 2003). The targeting construct was generated using *pOSfrt* (Caron and Smithies, 2001) as the backbone, which contains (a) a 4.4-kb PCR-generated fragment from genomic DNA that includes the *BMPER* promoter; (b) a 700-bp cDNA encoding EGFP (Clontech Laboratory Inc.); (c) a 300-bp bovine growth hormone poly(A) addition region; and (d) a 2.0-kb PCR-generated genomic fragment from second intron of the *BMPER* gene. Embryonic stem (ES) cells (129/ola) were electroporated with the target construct. ES colonies that were G418/ganciclovir resistant were identified by the PCR-based assay. Homologous recombination was confirmed by Southern analysis using both 5′ and 3′ diagnostic probes. The targeted ES cells were injected into C57BL/6 blastocysts (Dai et al., 2003). Male chimeras were mated to wild-type C57BL/6 females to establish an isogenic line, and all experiments were conducted on the resulting hybrid background.

Genotyping of *Bmper* mutant mice

Genomic DNA of Bmper-deficient mice was isolated and digested with HpaI (5′ probe) and NheI (3′ probe) to identify wild-type and targeted alleles. *Bmper* homologous mutants were generated by timed heterozygous matings. A PCR analysis has been developed to genotype the embryos and pups. PCR samples were denatured in 95°C for 60 s, and then subjected to 35 cycles of three-step amplification, a 30-s 94°C denaturation, 30-s 68°C annealing, and 45-s 72°C extension step. A 608-bp product (primers berwtf and bergtr) represents the wild-type allele and a 455-bp product (primers berkof and bergtr) indicates the target allele. PCR primers: berwtf, 5′-CTGCATCCACCCCTGTAAGTTTCTAG-3′; berkof, 5′-gtcctctgatggtcaaagtcctg-3′; bergtr, 5′-CCAAGCCCAACGCTCCCTGCTGAAATCC-3′.

Southern blotting analysis

Southern blotting analysis was performed as previously described (Matzuk et al., 1992). Genomic DNA was digested with either HpaI or NheI and electrophoresed in a 1% agarose gel. Both 5′ and 3′ probe were labeled with α-[^{32}P]deoxycytidine triphosphate by random oligopriming. Membranes containing DNA have hybridized with labeled probes in 65°C for 1 h. The locations of radioactive probe hybridization on membrane were detected by autoradiography.

Statistical methods

Means ± SEM and a one-way analysis of variance were used for all figures that required statistical measurements. A multiple comparison procedure was used, using the Tukey method to determine statistical significance between groups.

Online supplemental material

Fig. S1 support endocytic studies in Fig. 3 through acid wash and Bmp4 neutralization experiments. Fig. S2 shows the strategy for deleting *Bmper* in ES cells and in mice. Figure S3 shows the immunohistochemistry for GFP to support the *Bmper* null phenotype in mice lung from Fig. 7. Online supplemental material is available at http://www.jcb.org/cgi/content/full/jcb.200808064/DC1.

We thank Vicky Madden and the Microscopy Services Laboratory of the Department of Pathology and Laboratory Medicine for assistance with electron microscopy studies. We thank William C. Sessa for the lung endothelial cells null for caveolin-1. We also thank Andrea Portbury for her critical review of the manuscript.

This work was supported by National Institutes of Health grants HL 61656, HL 03658, and HL 072347 to C. Patterson; a Canadian Institute for Health Research grant 178082 to L. Attisano; and a postdoctoral fellowship from the American Heart Association to R. Kelley.

The authors have no conflicting financial interests.

Submitted: 12 August 2008
Accepted: 23 January 2009

References

Ambrosio, A.L., V.F. Taelman, H.X. Lee, C.A. Metzinger, C. Coffinier, and E.M. De Robertis. 2008. Crossveinless-2 Is a BMP feedback inhibitor that binds Chordin/BMP to regulate *Xenopus* embryonic patterning. *Dev. Cell.* 15:248–260.

Balemans, W., and W. Van Hul. 2002. Extracellular regulation of BMP signaling in vertebrates: a cocktail of modulators. *Dev. Biol.* 250:231–250.

Bellusci, S., R. Henderson, G. Winnier, T. Oikawa, and B.L. Hogan. 1996. Evidence from normal expression and targeted misexpression that bone morphogenetic protein (Bmp-4) plays a role in mouse embryonic lung morphogenesis. *Development.* 122:1693–1702.

Binnerts, M.E., X. Wen, K. Cante-Barrett, J. Bright, H.T. Chen, V. Asundi, P. Sattari, T. Tang, B. Boyle, W. Funk, and F. Rupp. 2004. Human Crossveinless-2 is a novel inhibitor of bone morphogenetic proteins. *Biochem. Biophys. Res. Commun.* 315:272–280.

Bucci, C., P. Thomsen, P. Nicoziani, J. McCarthy, and B. van Deurs. 2000. Rab7: a key to lysosome biogenesis. *Mol. Biol. Cell.* 11:467–480.

Caron, K.M., and O. Smithies. 2001. Extreme hydrops fetalis and cardiovascular abnormalities in mice lacking a functional Adrenomedullin gene. *Proc. Natl. Acad. Sci. USA.* 98:615–619.

Choi, M., R.W. Stottmann, Y.P. Yang, E.N. Meyers, and J. Klingensmith. 2007. The bone morphogenetic protein antagonist noggin regulates mammalian cardiac morphogenesis. *Circ. Res.* 100:220–228.

Coles, E., J. Christiansen, A. Economou, M. Bronner-Fraser, and D.G. Wilkinson. 2004. A vertebrate crossveinless 2 homologue modulates BMP activity and neural crest cell migration. *Development.* 131:5309–5317.

Conley, C.A., R. Silburn, M.A. Singer, A. Ralston, D. Rohwer-Nutter, D.J. Olson, W. Gelbart, and S.S. Blair. 2000. Crossveinless 2 contains cysteine-rich domains and is required for high levels of BMP-like activity during the formation of the cross veins in *Drosophila*. *Development.* 127:3947–3959.

Dai, Q., C. Zhang, Y. Wu, H. McDonough, R.A. Whaley, V. Godfrey, H.H. Li, N. Madamanchi, W. Xu, L. Neckers, et al. 2003. CHIP activates HSF1 and confers protection against apoptosis and cellular stress. *EMBO J.* 22:5446–5458.

Degnin, C., F. Jean, G. Thomas, and J.L. Christian. 2004. Cleavages within the prodomain direct intracellular trafficking and degradation of mature bone morphogenetic protein-4. *Mol. Biol. Cell.* 15:5012–5020.

Di Guglielmo, G.M., C. Le Roy, A.F. Goodfellow, and J.L. Wrana. 2003. Distinct endocytic pathways regulate TGF-beta receptor signalling and turnover. *Nat. Cell Biol.* 5:410–421.

Entchev, E.V., A. Schwabedissen, and M. Gonzalez-Gaitan. 2000. Gradient formation of the TGF-beta homolog Dpp. *Cell.* 103:981–991.

Hartung, A., K. Bitton-Worms, M.M. Rechtman, V. Wenzel, J.H. Boergermann, S. Hassel, Y.I. Henis, and P. Knaus. 2006. Different routes of bone morphogenic protein (BMP) receptor endocytosis influence BMP signaling. *Mol. Cell. Biol.* 26:7791–7805.

Hollnagel, A., V. Oehlmann, J. Heymer, U. Ruther, and A. Nordheim. 1999. Id genes are direct targets of bone morphogenetic protein induction in embryonic stem cells. *J. Biol. Chem.* 274:19838–19845.

Ikeya, M., M. Kawada, H. Kiyonari, N. Sasai, K. Nakao, Y. Furuta, and Y. Sasai. 2006. Essential pro-Bmp roles of crossveinless 2 in mouse organogenesis. *Development.* 133:4463–4473.

Kamimura, M., K. Matsumoto, K. Koshiba-Takeuchi, and T. Ogura. 2004. Vertebrate crossveinless 2 is secreted and acts as an extracellular modulator of the BMP signaling cascade. *Dev. Dyn.* 230:434–445.

Larrain, J., M. Oelgeschlager, N.I. Ketpura, B. Reversade, L. Zakin, and E.M. De Robertis. 2001. Proteolytic cleavage of Chordin as a switch for the dual activities of Twisted gastrulation in BMP signaling. *Development.* 128:4439–4447.

Lee-Hoeflich, S.T., C.G. Causing, M. Podkowa, X. Zhao, J.L. Wrana, and L. Attisano. 2004. Activation of LIMK1 by binding to the BMP receptor, BMPRII, regulates BMP-dependent dendritogenesis. *EMBO J.* 23:4792–4801.

Lin, M.I., J. Yu, T. Murata, and W.C. Sessa. 2007. Caveolin-1-deficient mice have increased tumor microvascular permeability, angiogenesis, and growth. *Cancer Res.* 67:2849–2856.

Matzuk, M.M., M.J. Finegold, J.G. Su, A.J. Hsueh, and A. Bradley. 1992. Alpha-inhibin is a tumour-suppressor gene with gonadal specificity in mice. *Nature.* 360:313–319.

Michos, O., L. Panman, K. Vintersten, K. Beier, R. Zeller, and A. Zuniga. 2004. Gremlin-mediated BMP antagonism induces the epithelial-mesenchymal feedback signaling controlling metanephric kidney and limb organogenesis. *Development.* 131:3401–3410.

Moser, M., O. Binder, Y. Wu, J. Aitsebaomo, R. Ren, C. Bode, V.L. Bautch, F.L. Conlon, and C. Patterson. 2003. BMPER, a novel endothelial cell precursor-derived protein, antagonizes bone morphogenetic protein signaling and endothelial cell differentiation. *Mol. Cell. Biol.* 23:5664–5679.

Mukherjee, S., M. Tessema, and A. Wandinger-Ness. 2006. Vesicular trafficking of tyrosine kinase receptors and associated proteins in the regulation of signaling and vascular function. *Circ. Res.* 98:743–756.

Ralston, A., and S.S. Blair. 2005. Long-range Dpp signaling is regulated to restrict BMP signaling to a crossvein competent zone. *Dev. Biol.* 280:187–200.

Ren, R., P.C. Charles, C. Zhang, Y. Wu, H. Wang, and C. Patterson. 2007. Gene expression profiles identify a role for cyclooxygenase 2-dependent prostanoid generation in BMP6-induced angiogenic responses. *Blood.* 109:2847–2853.

Rentzsch, F., J. Zhang, C. Kramer, W. Sebald, and M. Hammerschmidt. 2006. Crossveinless 2 is an essential positive feedback regulator of Bmp signaling during zebrafish gastrulation. *Development.* 133:801–811.

Serpe, M., D. Umulis, A. Ralston, J. Chen, D.J. Olson, A. Avanesov, H. Othmer, M.B. O'Connor, and S.S. Blair. 2008. The BMP-binding protein Crossveinless 2 is a short-range, concentration-dependent, biphasic modulator of BMP signaling in *Drosophila*. *Dev. Cell.* 14:940–953.

Srinivasan, S., K.E. Rashka, and E. Bier. 2002. Creation of a Sog morphogen gradient in the *Drosophila* embryo. *Dev. Cell.* 2:91–101.

Thuveson, M., and E. Fries. 2000. The low pH in trans-Golgi triggers autocatalytic cleavage of pre-alpha-inhibitor heavy chain precursor. *J. Biol. Chem.* 275:30996–31000.

Valdimarsdottir, G., M.J. Goumans, A. Rosendahl, M. Brugman, S. Itoh, F. Lebrin, P. Sideras, and P. ten Dijke. 2002. Stimulation of Id1 expression by bone morphogenetic protein is sufficient and necessary for bone morphogenetic protein-induced activation of endothelial cells. *Circulation.* 106:2263–2270.

Weaver, M., J.M. Yingling, N.R. Dunn, S. Bellusci, and B.L. Hogan. 1999. Bmp signaling regulates proximal-distal differentiation of endoderm in mouse lung development. *Development.* 126:4005–4015.

Weaver, M., N.R. Dunn, and B.L. Hogan. 2000. Bmp4 and Fgf10 play opposing roles during lung bud morphogenesis. *Development.* 127:2695–2704.

Yi, H., J. Leunissen, G. Shi, C. Gutekunst, and S. Hersch. 2001. A novel procedure for pre-embedding double immunogold-silver labeling at the ultrastructural level. *J. Histochem. Cytochem.* 49:279–284.

Zhang, J.L., Y. Huang, L.Y. Qiu, J. Nickel, and W. Sebald. 2007. von Willebrand factor type C domain-containing proteins regulate bone morphogenetic protein signaling through different recognition mechanisms. *J. Biol. Chem.* 282:20002–20014.